HHS Public Access

Author manuscript

J Mol Biol. Author manuscript; available in PMC 2016 November 06.

Published in final edited form as:

J Mol Biol. 2015 November 6; 427(22): 3491–3500. doi:10.1016/j.jmb.2015.07.010.

Acidic residues in the Hfq chaperone increase the selectivity of sRNA binding and annealing

Subrata Panja[†,1], **Andrew Santiago-Frangos**[†,2], **Daniel J. Schu**[3,¶], **Susan Gottesman**[3], and **Sarah A. Woodson**[1,2,*]

[1]T.C. Jenkins Department of Biophysics, Johns Hopkins University, 3400 N. Charles St., Baltimore, MD 21218, USA

[2]CMDB Program, Johns Hopkins University, 3400 N. Charles St., Baltimore, MD 21218, USA

[3]Laboratory of Molecular Biology, Building 37, Room 5132, National Cancer Institute, Bethesda, MD 20892 USA

Abstract

Hfq facilitates gene regulation by small non-coding RNAs (sRNAs), thereby affecting bacterial attributes such as biofilm formation and virulence. *E. coli* Hfq recognizes specific U-rich and AAN motifs in sRNAs and target mRNAs, after which an arginine patch on the rim promotes base pairing between their complementary sequences. In the cell, Hfq must discriminate between many similar RNAs. Here, we report that acidic amino acids lining the sRNA binding channel between the inner pore and rim of the Hfq hexamer contribute to the selectivity of Hfq's chaperone activity. RNase footprinting, *in vitro* binding and stopped-flow fluorescence annealing assays showed that alanine substitution of D9, E18 or E37 strengthened RNA interactions with the rim of Hfq and increased annealing of non-specific or U-tailed RNA oligomers. Although the mutants were less able than WT Hfq to anneal sRNAs with wild type *rpoS* mRNA, the D9A mutation bypassed recruitment of Hfq to an $(AAN)_4$ motif in *rpoS*, both *in vitro* and *in vivo*. These results suggest that acidic residues normally modulate access of RNAs to the arginine patch. We propose that this selectivity limits indiscriminate target selection by *E. coli* Hfq, and enforces binding modes that favor genuine sRNA and mRNA pairs.

Graphical Abstract

[*]Correspondence to swoodson@jhu.edu; tel. 410-516-2015; FAX 410-516-4118.
[†]These authors contributed equally to this work
[¶]Current address: Food and Drug Administration, Silver Spring, MD. 20993-0002

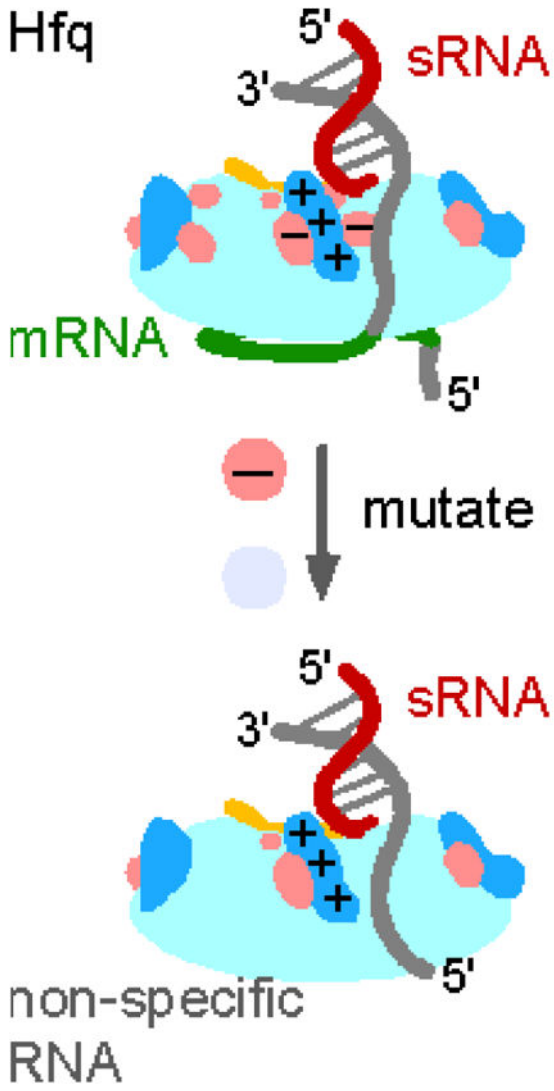

Keywords

Hfq; non-coding RNA; RNA chaperone; RNA-protein interactions; molecular beacon; RNA annealing; sRNA; RNase footprinting; Sm protein

INTRODUCTION

In bacteria, small RNAs (sRNAs) regulate gene expression during environmental stress conditions like cold shock, oxidative stress, osmotic shock and quorum sensing [1; 2; 3]. Transacting sRNAs activate or repress expression of certain genes by base pairing with the 5′-UTR of the target mRNAs [4], either masking or exposing the Shine-Dalgarno ribosome binding site, or recruiting RNase E for mRNA turnover [5; 6]. In Gram-negative bacteria, sRNAs typically act together with the RNA chaperone protein Hfq [6; 7], which accelerates annealing of complementary RNA strands and stabilizes sRNA-mRNA duplexes [8; 9; 10; 11].

The observed regulation depends on the specificity of these complexes, as different sRNAs must compete for binding to Hfq and their proper mRNA target.

Bacterial Hfq is a member of the Sm/Lsm super-family that forms a homo-hexamer ring with two distinct single-stranded RNA binding surfaces [7] (Fig. 1a). The proximal face of Hfq binds to U-rich RNA sequences found in sRNAs while the distal face of Hfq binds to AAN motifs found in the 5′-UTR of mRNAs [12; 13; 14]. In addition, a patch of highly conserved arginine residues on the rim of Hfq binds U-rich regions of the mRNA and sRNA body [15; 16; 17] and is thought to be responsible for the RNA annealing activity of Hfq [18].

In our working model for the Hfq annealing cycle, sRNAs and mRNAs are recruited to the proximal and distal surfaces of Hfq through specific recognition of U and A-rich motifs. When Hfq forms a ternary complex with two complementary RNAs, interactions with the positively charged arginine patch accelerate base pairing between the anti-sense regions [18]. In addition, simultaneous interactions with different RNA-binding surfaces of Hfq distort sRNA and mRNA structures, orienting them for anti-sense annealing [15; 19; 20].

The arginine patch in Hfq is surrounded by four conserved acidic residues D9, E18, E37 and D40 in *E. coli* Hfq (Fig. 1a). Invariant D9 and D40 lie on either side of a channel that sRNAs use as a passage between the inner proximal face RNA binding site and the arginine patch [15; 17], while the moderately conserved E18 and E37 flank the arginine patch on the distal rim of Hfq (Fig. 1a). Although negatively charged residues are not expected to interact with RNA, replacement of the almost universally conserved D9 with alanine impaired the ability of Hfq to support regulation of *cirA* by OmrA sRNA [21], *chiP* by ChiX sRNA and *sdhCDAB* by RyhB sRNA in *E. coli* [22]. These results indicated that D9 is important for sRNA binding to Hfq, or for regulation of these target genes by sRNAs.

Here we show that removing D9 or other acidic residues makes the Hfq rim more accessible to unstructured RNAs, improving the ability of Hfq to act on RNAs lacking a specific Hfq binding site. Further *in vitro* and *in vivo* assays confirmed that mutating acidic residues overrides the requirement for AAN motifs which normally recruit Hfq to *rpoS* mRNA for riboregulation. The D9A mutation was even found to rescue Hfq alleles defective for RNA binding to the rim and distal face. The results presented here suggest that the acidic residues normally act to limit RNA binding to arginine patch, thereby increasing the selectivity of Hfq's chaperone function.

RESULTS

Conserved acidic residues regulate the accessibility of the rim

Each of the four acidic side chains on the proximal face of Hfq was replaced with alanine (D9A, E18A, E37A and D40A) and the variants tested for RNA binding and annealing activity. The D40A mutant protein could not form a stable hexamer as previously reported [22] and was therefore not analyzed further. Equilibrium binding constants for oligoribonucleotides and sRNAs were measured using fluorescence anisotropy and electrophoretic gel mobility shift assays (EMSA), respectively (Table 1).

We compared RNAs that primarily bind the rim of Hfq, or that interact with both the inner pore and outer rim of the proximal surface. An unstructured 16 nt RNA derived from the body of DsrA [23], D16, has six internal uridines and is thought to mainly interact with the proximal rim [18]. Wild type (WT) *E. coli* Hfq binds FAM-labeled D16 (D16-FAM) with K_d = 67 nM (Hfq monomer) in TNK buffer at 30°C. The D9A and E18A variants bound D16-FAM more tightly than the WT protein, with dissociation constants of 47 nM and 24 nM, respectively.

Natural sRNAs end in 3′ uridines that tightly bind the inner proximal surface of Hfq, in addition to internal uridines and stem-loops that interact with the rim [24; 25]. The D9A and E18A mutations weakened overall binding of DsrA sRNA about twofold compared to WT Hfq (Table 1; Fig. S1). When the 3′ terminal uridines were removed (DsrAΔU_6), binding to WT Hfq became almost six-fold weaker (Table I). Thus, the WT Hfq-DsrA complex is stabilized more by interactions between the U-tail and the proximal face than the rim. By contrast, removing the U-tail had a much smaller effect on the overall affinity of DsrA for Hfq:D9A, raising the K_d less than twofold (Table I). As a result, the tail-less sRNA actually bound Hfq:D9A more tightly than it bound WT Hfq. We conclude that the D9A mutation increases RNA binding to the rim, perhaps owing to the increased net positive charge, while weakening the ability of structured sRNAs to simultaneously contact the rim and the inner pore of Hfq.

To directly test whether removing an acidic residue strengthens RNA interactions with the rim of Hfq, we monitored the ability of different RNAs to quench the fluorescence of a tryptophan introduced at residue 38 near the arginine patch (Fig. 2a; Fig S2a). This tryptophan substitution reports interactions with the rim of Hfq, as short RNAs that cannot bind the rim do not reduce the emission intensity [18]. This mutation does not impair sRNA-mRNA annealing *in vitro* (Fig. S2b). All of the RNAs tested quenched the tryptophan fluorescence signal of Hfq:S38W by 15–20%. These RNAs were oligo C, an unstructured 16-mer that binds the Hfq rim non-specifically, oligo C-U_6 (CU), which interacts with the proximal face and rim, DsrA sRNA and ArcZ56 sRNA. The D9A and E18A mutations resulted in stronger quenching of the tryptophan signal by all of the RNAs tested (Fig. 2b), consistent with stronger binding of RNAs to the rim of Hfq when a negatively charged side chain is removed.

Acidic residues contribute to sRNA recognition

To ask whether the acidic residues influence how Hfq interacts with specific sRNA sequences, partial digestion with RNase I_f was used to probe the structure of ^{32}P-labeled DsrA with and without Hfq. WT Hfq protects single-stranded nt 25–28 and U's 32–38 in the body of DsrA while enhancing cleavage of nt 51–53 in loop 2 (black labels in Fig. 3), as reported previously [8; 26]. Hfq:D9A protected DsrA much more strongly than WT Hfq (red labels in Fig. 3). The E18A and E37A Hfq mutants protected the same regions of DsrA, but to a degree more like that of WT Hfq (blue and green traces, Fig. 3b inset). Since the body of DsrA is thought to interact with the rim of Hfq [15], the footprinting results also indicate that the D9A mutation especially increases RNA binding to the rim of Hfq, even though the sRNA-Hfq complex is less stable overall owing to weaker interactions with the U_6 tail

(Table 1). The loss of enhancements in stem-loop I and loops II and III further suggest that Hfq:D9A cannot interact with DsrA as precisely as the WT protein (Fig. 3c).

Acidic residues increase annealing of non-specific and U-rich RNAs

Since the arginine patch on the rim is essential for Hfq's chaperone activity [18], we asked whether the loss of adjacent acidic residues could affect the annealing of complementary RNA strands. To compare the chaperone activity of each Hfq variant, the annealing kinetics of a molecular beacon and 16 nt target RNAs were measured by stopped-flow fluorescence (Fig. 4a). Wild type Hfq speeds up base pairing between a molecular beacon and unstructured RNAs, such as oligo C, which bind the Hfq rim non-specifically (Fig. S3) [27]. This acceleration reached a maximum at 300 nM Hfq, which equaled one Hfq hexamer per RNA pair (Fig. 4b, solid blue). Hfq acts most efficiently, however, when one of the RNA strands contains an A_{18} tail that binds the distal face of Hfq, increasing the annealing rate 20 to 60 fold (Fig. 4b, solid black) [28].

When the A-tailed target RNA (oligo CA) was recruited to the distal face of Hfq, the D9A mutation reduced the annealing rate less than twofold (Fig. 4b; compare black open and closed circles). A subtle effect on the A-tailed target was expected because the D9 residue is located on the proximal face of Hfq. Far more surprising was that the D9A mutation greatly improved the annealing rate when a U-tailed target RNA (oligo CU) was recruited to the proximal face of Hfq (Fig. 4b; compare red open and closed circles). Similar increases in annealing rate were observed for oligo C, which lacks a specific Hfq binding site (Fig. 4b; compare blue open and closed circles). Parallel changes in the annealing kinetics were observed for the E18A and E37A variants (Fig. 4c), in that each of these acidic residue Hfq mutations reduced the preference for annealing A-tailed RNA substrates over U-tailed (CU) and untailed (C) substrates (Fig 4c; compare black bar to red and blue bars).

Loss of acidic residues makes sRNA-mRNA annealing less efficient

In contrast to unstructured oligonucleotides, natural sRNAs and mRNAs must make specific contacts with the proximal pore and the rim. We next tested whether the acidic residues affect the ability of Hfq to facilitate annealing of DsrA and ArcZ sRNAs to *rpoS* mRNA in vitro (Fig. 5a). As expected, DsrA and *rpoS* mRNA base paired with each other about 60 times faster with WT Hfq than without Hfq. All of the Hfq variants could facilitate sRNA annealing to *rpoS* mRNA, but the reaction became less efficient when an acidic side chain was mutated. For DsrA, the amplitude of the Hfq-dependent burst phase was lowered from 50% for WT Hfq to 33%, 43% and 34% for Hfq:D9A, E18A and E37A, respectively (Fig. 5b).

A 56 nt form of ArcZ sRNA (ArcZ56) requires Hfq to base pair with *rpoS* mRNA [29; 30], unlike DsrA which slowly base pairs with rpoS in the absence of Hfq (grey lines, Fig. 5a, b). Mutations in the acidic residues did not change the initial burst, but they did diminish the amount of ArcZ56•Hfq•*rpoS* product formed after 4 minutes, from 80% in the presence of WT Hfq to only 64%, 47% and 55% with D9A, E18A and E37A Hfq, respectively. One explanation for these results is that tighter interactions with the rim make the ArcZ56-*rpoS* duplex less able to cycle off Hfq after base pairing has occurred, leading to refolding of *rpoS*

and displacement of ArcZ56. Alternatively, the acidic residue mutants may not fold *rpoS* mRNA correctly for sRNA annealing, reducing the yield of sRNA-mRNA-Hfq complex for both DsrA and ArcZ56.

D9A mutation bypasses the requirement for *rpoS* AAN motifs

Up-regulation of *rpoS* by sRNAs depends on recruitment of Hfq to $(AAN)_4$, A_6 and U_5 motifs within the *rpoS* 5′ UTR (Fig. 6a), which are needed for Hfq to promote sRNA-mRNA base pairing *in vivo* and *in vitro* [20; 29; 31]. Mutagenesis of either the $(AAN)_4$ or U_5 motifs alone, or all three motifs together (ΔΔΔ), lowered the burst of DsrA annealing by WT Hfq from 67% with *rpoS301* to 14% with ΔΔΔ*rpoS301* (Fig. 6b, white and grey bars). In contrast, mutagenesis of canonical Hfq binding motifs in *rpoS* mRNA had no effect on DsrA annealing by Hfq:D9A (Fig. 6b, red bars).

We next asked whether D9 affects the requirements for *rpoS* mRNA regulation by sRNAs *in vivo*. Over-expression of DsrA and ArcZ sRNAs from an IPTG-inducible promoter increased translation of an *rpoS::lacZ* fusion in the *E. coli* chromosome to a similar extent in strains containing wild type or mutant *hfq* alleles in the bacterial chromosome (Fig. S4). In fact, we observed slightly greater up-regulation of *rpoS* by ArcZ in strains expressing Hfq:D9A, E18A or E37A compared to WT Hfq. These results were consistent with previous studies, which found that D9A was more important for negative regulation than positive regulation of *rpoS*, and had little effect on the accumulation of ArcZ and DsrA sRNAs in *E. coli* [22]. Because the *rpoS-lacZ* mRNA was strongly induced by arabinose in these experiments, however, deficiencies in Hfq binding to the mRNA may have been masked [22].

To test whether the D9A allele also bypassed the need for Hfq to bind the *rpoS* AAN motif *in vivo*, we assayed translation of a WT *rpoS-lacZ* fusion on MacConkey agar plates. In the absence of a plasmid (akin to the vector control in Fig. S4b), *rpoS-lacZ* expression depends on endogenous levels of DsrA, ArcZ and RprA [30]. Deletion of the $(AAN)_4$ motif alone, $(AAN)_4$ and A_6 (ΔΔ), or all three motifs (ΔΔΔ) lowered the expression of the *rpoS* fusion in the presence of WT Hfq (WT sectors in Fig. 6c). However, the deleterious effects of these *rpoS* mutations were suppressed when Hfq carried the D9A allele (D9A sectors in Fig. 6c), in agreement with the *in vitro* annealing results (Fig. 6b). The ability of Hfq:D9A to suppress deletion of the *rpoS* $(AAN)_4$ motif was also seen when mutants in the rim or distal site were combined with a deletion of the $(AAN)_4$ or deletion of all three motifs (Fig. S5). Thus, the D9A mutation not only compensates for weaker rim binding, in agreement with our tryptophan quenching data, but surprisingly bypasses the need to recruit Hfq to the *rpoS* mRNA via the upstream $(AAN)_4$ motif.

DISCUSSION

E. coli encodes about 100 different sRNAs that regulate up to 700 genes [32; 33]. Although not all sRNAs are expressed simultaneously, the Hfq chaperone must still discriminate between sRNAs and other transcripts, while promoting base pairing with a diversity of mRNA targets. This is largely accomplished by specific recognition of U-rich and A-rich sequence motifs present in natural substrates of Hfq. It has been recently recognized, however, that natural RNAs interact with multiple surfaces of Hfq in a manner that likely depends on the

RNA secondary structure. These multi-lateral interactions trigger structural rearrangements needed for efficient sRNA-mRNA recognition. For example, single-stranded 3′ uridines anchor sRNAs to the inner pore of the proximal face, while the body of many sRNAs binds the rim of Hfq [15; 18]. Hfq restructures the *rpoS* mRNA leader even more dramatically by recognizing an upstream $(AAN)_4$ motif and the U_5 motif downstream of the sRNA binding site [20]. These interactions fold the *rpoS* mRNA 5′-UTR into a compact structure [20], partially melting the inhibitory stem containing the sRNA target sequence [34].

Our results suggest that acidic residues on the proximal face and rim act as “gatekeepers” that increase the selectivity of RNA interactions with arginine patch. Tryptophan quenching data showed that removal of an acidic side chain allows oligonucleotides and sRNAs to bind the rim of Hfq more tightly (Fig. 2). Similarly, Hfq:D9A protected internal residues of DsrA from ribonuclease digestion more strongly than WT Hfq protected them (Fig. 3). Mutations in acidic residues could improve RNA binding to the rim by simply making the rim more positively charged, or by changing the structure of Hfq to make the rim more accessible.

Tighter RNA binding to the rim appears to shift sRNA recognition from the inner proximal pore, which is highly selective for uridine, to the rim, which is less sequence-specific. Although the uridines at the 3′ end of DsrA are important for the stability of the complex with the WT protein, removing the U-tail had little effect on the stability of the Hfq:D9A-DsrA complex (Table 1). In addition, Hfq:D9A perturbed interactions with DsrA stem-loops II and III (Fig. 3). The rim of Hfq has been long reported to bind double-stranded RNA [35; 36], and is likely important for folding structured RNAs around Hfq in a manner that promotes sRNA-mRNA annealing and gene regulation [17; 20].

This shift toward stronger RNA interactions at the rim may explain why acidic residue mutations allow Hfq to bypass AAN motifs, which are normally required for Hfq to act on *rpoS* mRNA [29; 31] and other targets. In our annealing assays with unstructured oligonucleotides, Hfq:D9A was as active on non-specific and U-tailed RNAs as on A-tailed RNAs, while WT Hfq is far more active on RNAs containing an A-tail (Fig. 4). Similarly, increased non-specific binding of RNAs at the rim enables Hfq:D9A to form an alternative complex with *rpoS* which is modestly less active than the WT Hfq·*rpoS* complex but does not depend on interactions with the $(AAN)_4$ and A_6 motifs both *in vitro* and *in vivo*. Additionally, the D9A mutation overcame the deleterious effects of mutations on the rim (R16A) and distal face (Y25D and K31A) on *rpoS* up-regulation in the absence of the AAN motifs *in vivo* (Fig. S5), further indicating that it bypasses the need for specific recruitment of Hfq to AAN motifs. Together our results suggest that loss of a negatively charged side chain allows Hfq to act on RNAs that lack specific U or A-rich binding sites.

Although replacement of an acidic residue makes Hfq a less discriminating chaperone, this is apparently detrimental to the function of certain sRNA-mRNA pairs. The Hfq D9A allele was first isolated for its failure to support negative regulation of *sdhC* by RyhB sRNA and negative regulation of *cirA* by OmrB [21], and in subsequent studies D9A was more deleterious for negative than positive regulation [22]. One possibility is that the mutant Hfq proteins fail to properly restructure both positive and negative mRNA targets for optimal base pairing with incoming sRNAs. These mutations could also weaken Hfq binding to

mRNA sequence motifs needed for translational repression. Alternatively, the shift from recognition of the sRNA 3′ end to the sRNA body may allow Hfq to prematurely dissociate from sRNA-mRNA complexes, also weakening repression. Finally, the higher expression of *rpoS::lacZ* in the absence of sRNA overexpression suggests that these Hfq mutations may upset the competition between native sRNAs, elevating *rpoS* translation by basal levels of ArcZ, DsrA or RprA sRNAs. Regardless of the mechanism, we conclude that conserved negative charges surrounding the rim RNA binding site unexpectedly contribute to selective recognition of sRNAs and their targets by Hfq.

MATERIALS AND METHODS

Hfq purification

Wild type Hfq was overexpressed and purified from *E. coli* BL21 (DE3) cells using a Hi-Trap Co^{2+} column (GE Healthcare) and UNO S6 ion-exchange column (Bio-Rad) as previously described [37]. Alignment of 145 non-redundant (<90% identity) Hfq sequences showed that D9 and D40 are almost invariant while E18 and E37 are moderately conserved. Hfq mutants (D9A, E18A, E37A, D40A, WT-S38W, D9A-S38W, and E18A-S38W) were made by QuikChange (Stratagene) and purified using the same protocol.

Fluorescence binding assays

Binding constants for Hfq and D16-FAM RNA were measured by fluorescence anisotropy as described before [23]. RNA binding to the rim was measured by changes in the fluorescence emission of a single tryptophan Hfq-S38W as previously described [18]. Contributions from the inner filter effect were determined by repeating the RNA titrations in buffer containing 1.25 M NaCl, which inhibits RNA binding. The percent quenching of the tryptophan fluorescence emission at 340 nm was calculated as $100\% \times \{(I_0 - I)/I_0 - (I_0' - I')/I_0'\}$, in which I_0 is the initial tryptophan emission in the absence of RNA, I is the emission in the presence of RNA, and I_0' and I' are the initial tryptophan emission and the emission in the presence of RNA in 1.25 M NaCl respectively.

RNase I_f footprinting

5′-^{32}P-DsrA (0.1 μM) and DsrA–Hfq complexes (8 μl) containing 1 μM Hfq monomer were prepared as described [8] and incubated 30 min at 30°C. Each sample was treated with 2 μl 1.25 U/μl of RNase I_f for 1 min at 37°C. Reactions were stopped by the addition of 10 μl buffered phenol. After phenol-chloroform extraction and ethanol precipitation, RNA pellets were redissolved in 6 μl formamide loading dye (90% (v/v) formamide, TBE, 0.1% (w/v) bromophenol blue, 0.1% (w/v) xylene cyanol) and subsequently loaded on an 8% polyacrylamide sequencing gel. Sequence ladders were obtained by nuclease digestion under denaturing conditions as described [38]. Band intensities were integrated with SAFA [39] and normalized to bands with constant intensity (nt 5–7) in different experiments.

Molecular beacon-target annealing kinetics

Reverse-phase HPLC purified RNA molecular beacon, 5′ FAM-GGUCCCCCACUCGA CUCACCA**C**CGGACC-DABCYL (Trilink Biotechnologies), was used without further purification. Target RNAs (Dharmacon) were purified as described previously [28]. The target

RNA sequences were oligo C, 5′GUGGUCAGUCGAGUGG3′; CU, oligo C plus U_6; CA, oligo C plus A_{18}. The annealing kinetics between the molecular beacon (50 nM) and target RNA (100 nM) in TNK buffer (10 mM Tris-HCl pH 7.5, 50 mM NaCl, 50 mM KCl) at 30°C was measured by an Applied Photophysics SX 18MV stopped-flow spectrometer as described previously [28; 40]. Reactions were performed with 0–1.5 μM Hfq monomer as shown in the figures.

Native gel mobility shift assays for rpoS RNA and sRNA

DsrA, ArcZ56 and rpoS301 RNA were transcribed *in vitro* [8]. Binding affinities of Hfq variants with ^{32}P labeled DsrA at 30°C were measured by a native gel shift assay as previously described [8]. The disappearance of labeled DsrA was plotted against Hfq monomer concentrations and subsequently fit to a Hill equation ($\theta = A\,[\mathrm{Hfq}]^n/([\mathrm{Hfq}]^n + K_d^n)$), in which θ is the fraction of DsrA bound to Hfq, A is the amplitude, K_d is the binding constant and n is the Hill co-efficient (Fig. S1). The association kinetics of ^{32}P-labeled *rpoS* mRNA 5′-UTR (rpoS301) with 200 nM sRNA in the presence of WT or mutant Hfq protein was measured by native gel mobility shift as described before [8; 29]. The fraction of counts in each lane corresponding to *rpoS*•sRNA duplex or *rpoS*•Hfq•sRNA ternary complex versus time was fit to a biphasic rate equation.

β-Galactosidase activity assay

A derivative of wild-type *E.coli* MG1655 in which the 5′-UTR of *rpoS* was fused to *lacZ*, downstream of a pBAD promoter, [29] was further modified by P1 phage transduction [41] to introduce chromosomal Hfq mutations. The mutants were constructed as previously described [22] and confirmed by sequencing (see Supplementary Table S1). These strains were transformed with pLac, pDsrA and pArcZ plasmids [30]. Overnight cultures were diluted into fresh LB containing arabinose (0.2%), ampicillin (100 μg/mL), and IPTG (100 μM) for 6 hours. OD_{600} and β-galactosidase activity were measured as described previously [29]. The specific activities were calculated by V_{max}/OD_{600} and were the average of three independent measurements. For plate assays, *E. coli* strains listed in Table S1 were grown overnight at 37°C on MacConkey agar containing 0.0001% arabinose, if not stated otherwise.

Supplementary Material

Refer to Web version on PubMed Central for supplementary material.

Acknowledgments

FUNDING

This work was supported by a grant from the National Institute of General Medicine [R01 GM46686 to S.W.] and in part by the Intramural Research Program of the National Cancer Institute, Center for Cancer Research (to S.G.)

The authors thank N. Majdalani and Y. Peng for technical help, and N. De Lay, G. Storz, T. Updegrove, and A. Zhang for discussion and comments..

References

1. Gottesman S, McCullen CA, Guillier M, Vanderpool CK, Majdalani N, Benhammou J, Thompson KM, FitzGerald PC, Sowa NA, FitzGerald DJ. Small RNA regulators and the bacterial response to stress. Cold Spring Harbor Symp Quant Biol. 2006; 71:1–11. [PubMed: 17381274]
2. Harris JF, Micheva-Viteva S, Li N, Hong-Geller E. Small RNA-mediated regulation of host-pathogen interactions. Virulence. 2013; 4:785–795. [PubMed: 23958954]
3. Kaberdin VR, Blasi U. Translation initiation and the fate of bacterial mRNAs. FEMS Microbiol Rev. 2006; 30:967–979. [PubMed: 16989654]
4. Storz G, Opdyke JA, Zhang A. Controlling mRNA stability and translation with small, noncoding RNAs. Curr Opin Microbiol. 2004; 7:140–144. [PubMed: 15063850]
5. Aiba H. Mechanism of RNA silencing by Hfq-binding small RNAs. Curr Opin Microbiol. 2007; 10:134–139. [PubMed: 17383928]
6. Vogel J, Luisi BF. Hfq and its constellation of RNA. Nat Rev Microbiol. 2011; 9:578–589. [PubMed: 21760622]
7. Weichenrieder O. RNA binding by Hfq and ring-forming (L)Sm proteins: A tradeoff between optimal sequence readout and RNA backbone conformation. RNA Biol. 2014; 11:537–549. [PubMed: 24828406]
8. Lease RA, Woodson SA. Cycling of the Sm-like protein Hfq on the DsrA small regulatory RNA. J Mol Biol. 2004; 344:1211–1223. [PubMed: 15561140]
9. Zhang A, Wassarman KM, Ortega J, Steven AC, Storz G. The Sm-like Hfq Protein Increases OxyS RNA Interaction with Target mRNAs. Mol Cell. 2002; 9:11–22. [PubMed: 11804582]
10. Moller T, Franch T, Hojrup P, Keene DR, Bachinger HP, Brennan RG, Valentin-Hansen P. Hfq: a bacterial Sm-like protein that mediates RNA-RNA interaction. Mol Cell. 2002; 9:23–30. [PubMed: 11804583]
11. Moll I, Leitsch D, Steinhauser T, Blasi U. RNA chaperone activity of the Sm-like Hfq protein. EMBO Rep. 2003; 4:284–289. [PubMed: 12634847]
12. Link TM, Valentin-Hansen P, Brennan RG. Structure of Escherichia coli Hfq bound to polyriboadenylate RNA. Proc Natl Acad Sci USA. 2009; 106:19292–19297. [PubMed: 19889981]
13. Schumacher MA, Pearson RF, Moller T, Valentin-Hansen P, Brennan RG. Structures of the pleiotropic translational regulator Hfq and an Hfq-RNA complex: a bacterial Sm-like protein. EMBO J. 2002; 21:3546–3556. [PubMed: 12093755]
14. Mikulecky PJ, Kaw MK, Brescia CC, Takach JC, Sledjeski DD, Feig AL. Escherichia coli Hfq has distinct interaction surfaces for DsrA, rpoS and poly(A) RNAs. Nat Struct Mol Biol. 2004; 11:1206–1214. [PubMed: 15531892]
15. Sauer E, Schmidt S, Weichenrieder O. Small RNA binding to the lateral surface of Hfq hexamers and structural rearrangements upon mRNA target recognition. Proc Natl Acad Sci USA. 2012; 109:9396–9401. [PubMed: 22645344]
16. Updegrove TB, Wartell RM. The influence of Escherichia coli Hfq mutations on RNA binding and sRNA*mRNA duplex formation in rpoS riboregulation. Biochim Biophys Acta. 2011; 1809:532–540. [PubMed: 21889623]
17. Dimastrogiovanni D, Frohlich KS, Bandyra KJ, Bruce HA, Hohensee S, Vogel J, Luisi BF. Recognition of the small regulatory RNA RydC by the bacterial Hfq protein. eLife. 2014:3.
18. Panja S, Schu DJ, Woodson SA. Conserved arginines on the rim of Hfq catalyze base pair formation and exchange. Nucleic Acids Res. 2013; 41:7536–7546. [PubMed: 23771143]
19. Geissmann TA, Touati D. Hfq, a new chaperoning role: binding to messenger RNA determines access for small RNA regulator. EMBO J. 2004; 23:396–405. [PubMed: 14739933]
20. Peng Y, Curtis JE, Fang X, Woodson SA. Structural model of an mRNA in complex with the bacterial chaperone Hfq. Proc Natl Acad Sci USA. 2014; 111:17134–17139. [PubMed: 25404287]
21. De Lay N, Gottesman S. Role of polynucleotide phosphorylase in sRNA function in Escherichia coli. RNA. 2011; 17:1172–1189. [PubMed: 21527671]

22. Zhang A, Schu DJ, Tjaden BC, Storz G, Gottesman S. Mutations in Interaction Surfaces Differentially Impact E. coli Hfq Association with Small RNAs and Their mRNA Targets. J Mol Biol. 2013; 425:3678–3697. [PubMed: 23318956]
23. Hopkins JF, Panja S, McNeil SA, Woodson SA. Effect of salt and RNA structure on annealing and strand displacement by Hfq. Nucleic Acids Res. 2009; 37:6205–6213. [PubMed: 19671524]
24. Ishikawa H, Otaka H, Maki K, Morita T, Aiba H. The functional Hfq-binding module of bacterial sRNAs consists of a double or single hairpin preceded by a U-rich sequence and followed by a 3′ poly(U) tail. RNA. 2012; 18:1062–1074. [PubMed: 22454537]
25. Sauer E, Weichenrieder O. Structural basis for RNA 3′-end recognition by Hfq. Proc Natl Acad Sci USA. 2011; 108:13065–13070. [PubMed: 21737752]
26. Brescia CC, Mikulecky PJ, Feig AL, Sledjeski DD. Identification of the Hfq-binding site on DsrA RNA: Hfq binds without altering DsrA secondary structure. RNA. 2003; 9:33–43. [PubMed: 12554874]
27. Hopkins JF, Panja S, Woodson SA. Rapid binding and release of Hfq from ternary complexes during RNA annealing. Nucleic Acids Res. 2011; 39:5193–5202. [PubMed: 21378124]
28. Panja S, Woodson SA. Hexamer to Monomer Equilibrium of E. coli Hfq in Solution and Its Impact on RNA Annealing. J Mol Biol. 2012; 417:406–412. [PubMed: 22326348]
29. Soper T, Mandin P, Majdalani N, Gottesman S, Woodson SA. Positive regulation by small RNAs and the role of Hfq. Proc Natl Acad Sci USA. 2010; 107:9602–9607. [PubMed: 20457943]
30. Mandin P, Gottesman S. Integrating anaerobic/aerobic sensing and the general stress response through the ArcZ small RNA. EMBO J. 2010; 29:3094–3107. [PubMed: 20683441]
31. Soper TJ, Woodson SA. The rpoS mRNA leader recruits Hfq to facilitate annealing with DsrA sRNA. RNA. 2008; 14:1907–1917. [PubMed: 18658123]
32. Raghavan R, Groisman EA, Ochman H. Genome-wide detection of novel regulatory RNAs in E. coli. Genome research. 2011; 21:1487–1497. [PubMed: 21665928]
33. Shinhara A, Matsui M, Hiraoka K, Nomura W, Hirano R, Nakahigashi K, Tomita M, Mori H, Kanai A. Deep sequencing reveals as-yet-undiscovered small RNAs in Escherichia coli. BMC genomics. 2011; 12:428. [PubMed: 21864382]
34. Soper TJ, Doxzen K, Woodson SA. Major role for mRNA binding and restructuring in sRNA recruitment by Hfq. RNA. 2011; 17:1544–1550. [PubMed: 21705431]
35. Lee T, Feig AL. The RNA binding protein Hfq interacts specifically with tRNAs. RNA. 2008; 14:514–523. [PubMed: 18230766]
36. Updegrove TB, Correia JJ, Galletto R, Bujalowski W, Wartell RM. E. coli DNA associated with isolated Hfq interacts with Hfq's distal surface and C-terminal domain. Biochim Biophys Acta. 2010; 1799:588–596. [PubMed: 20619373]
37. Peng Y, Soper TJ, Woodson SA. Positional effects of AAN motifs in rpoS regulation by sRNAs and Hfq. J Mol Biol. 2014; 426:275–285. [PubMed: 24051417]
38. Donis-Keller H, Maxam AM, Gilbert W. Mapping adenines, guanines, and pyrimidines in RNA. Nucleic Acids Res. 1977; 4:2527–2538. [PubMed: 409999]
39. Das R, Laederach A, Pearlman SM, Herschlag D, Altman RB. SAFA: semi-automated footprinting analysis software for high-throughput quantification of nucleic acid footprinting experiments. RNA. 2005; 11:344–354. [PubMed: 15701734]
40. Panja S, Woodson SA. Fluorescence reporters for Hfq oligomerization and RNA annealing. Methods Mol Biol. 2015; 1259:369–383. [PubMed: 25579597]
41. Silhavy, TJ. Experiments with gene fusions. Berman, ML.; Enquist, LW., editors. Cold Spring Harbor Laboratory; Cold Spring Harbor, N.Y: 1984.
42. Robinson KE, Orans J, Kovach AR, Link TM, Brennan RG. Mapping Hfq-RNA interaction surfaces using tryptophan fluorescence quenching. Nucleic Acids Res. 2014; 42:2736–2749. [PubMed: 24288369]

Highlights

- Hfq chaperones bacterial small non-coding RNAs during stress and pathogenesis
- *E. coli* Hfq normally selects cellular RNAs containing UUU or AAN sequence motifs
- Mutating acidic residues near the Hfq active site makes it less selective
- Asp 9 to Ala mutation bypasses recruitment of Hfq to AAN sites in mRNAs
- Acidic residues help Hfq discriminate between correct and non-specific targets

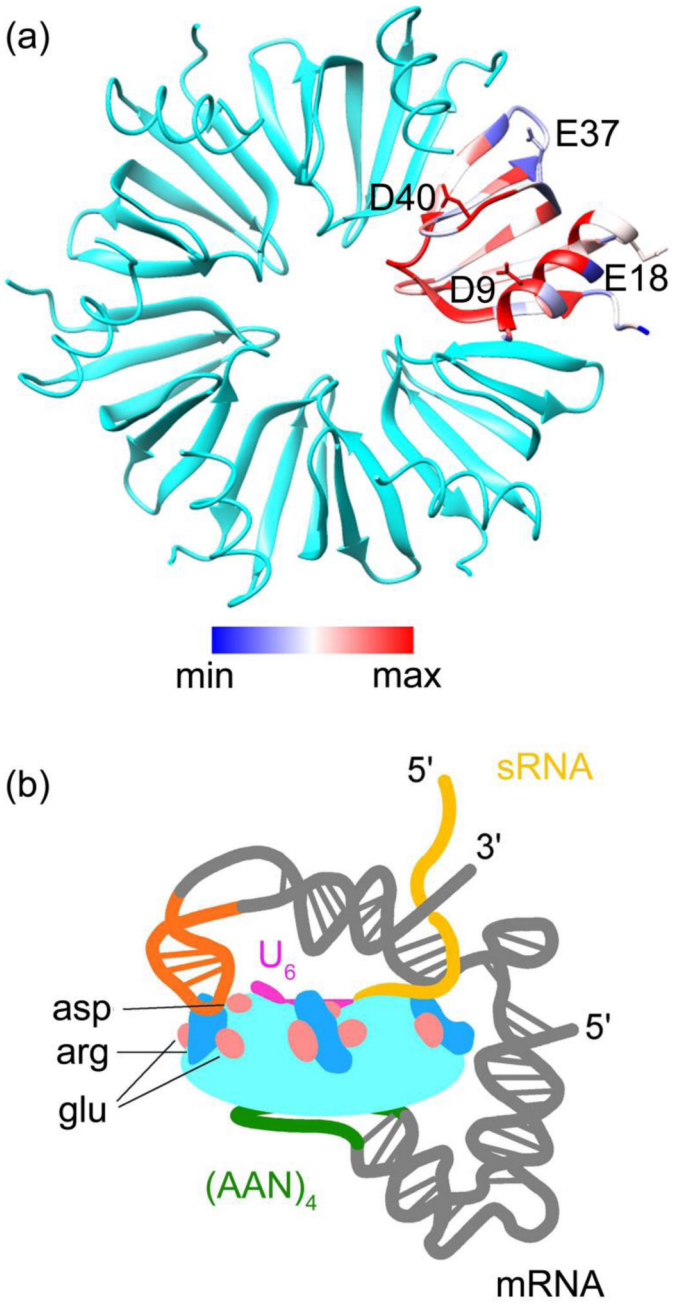

Fig. 1. Conserved acidic residues on the Hfq proximal surface

(a) Conservation scores of 145 Hfq sequence clusters were rendered from blue (minimum) to magenta (maximum) on one subunit of the hexamer (chain A; 1HK9). Acidic residues (D9, E18, E37 and D40) are shown as sticks. (b) Schematic representation of the sRNA-*rpoS*-Hfq ternary complex, based on solution data [20]. $(AAN)_4$ (green) and U_6 (magenta) motifs bind to the distal and proximal faces of Hfq, respectively. The U_5 loop in *rpoS* (orange) interacts with the rim. The complementary regions of the sRNA and mRNA interact with charged residues at the rim, which are needed to initiate base pairing.

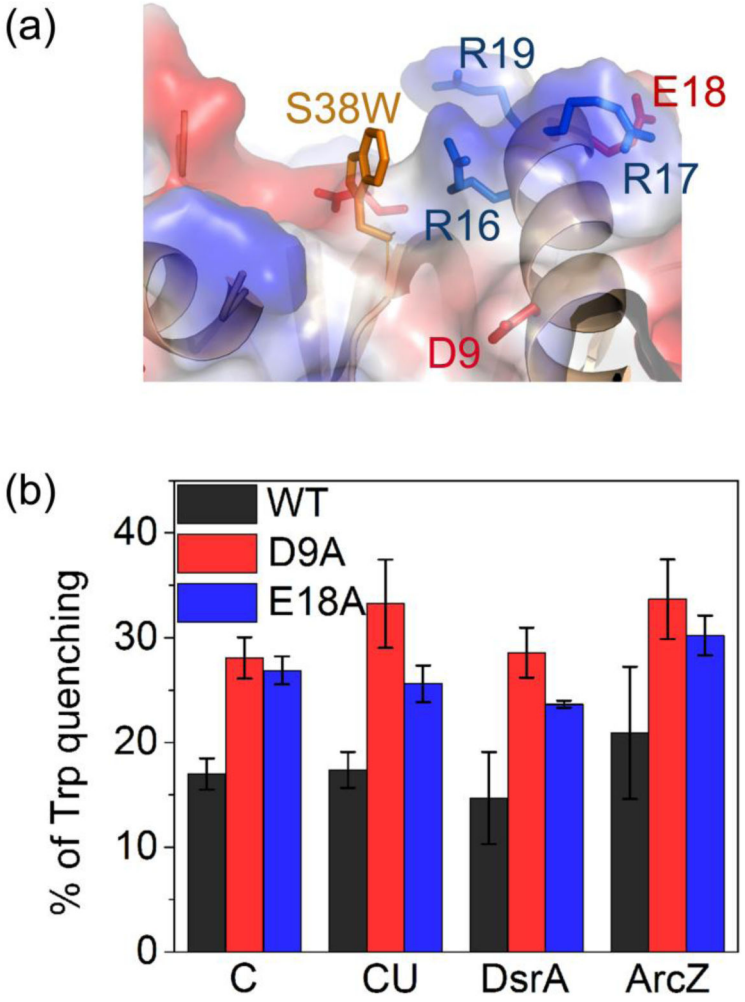

Fig. 2. Acidic side chains reduce RNA binding to the rim of Hfq

(a) A unique tryptophan at position 38 monitors RNA binding to the rim arginine patch. [18; 42] (b) Percent quenching of tryptophan emission in the presence of 100 nM RNA in TNK buffer at 30 °C, for Hfq variants shown in the key. These variants had similar (±20%) intrinsic fluorescence in the absence of RNA (Fig. S2c). Values were corrected for the inner filter effect (Methods and Fig. S2). Error bars represent the standard deviation from the mean of three independent trials.

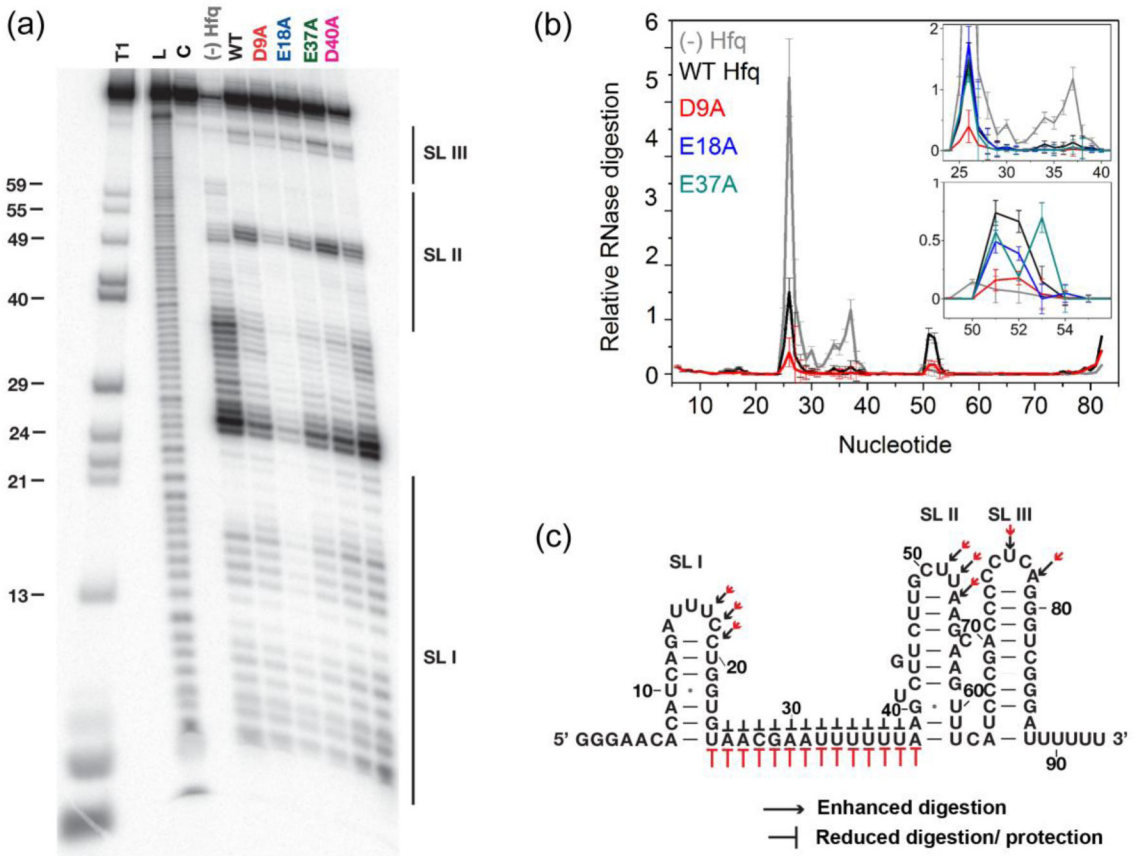

Fig. 3. Effect of acidic residues on DsrA recognition

(a) Ribonuclease I_f footprinting of 5′-^{32}P-labeled DsrA at 30 °C with no Hfq or with 10 μM Hfq monomer as shown. Lanes T1, L and C represent control reactions in urea with RNase T1 (T1), alkaline hydrolysis (L) and no treatment (C). The D40A variant forms unstable hexamers and these data were not analyzed further. (b) Relative RNase I_f digestion of nucleotides in DsrA. Gray, (−) Hfq; black, WT Hfq; red, D9A; (inset): blue, E18A; dark cyan, E37A. Lines and error bars trace the mean and S.D. of four trials (Methods). (c) Summary of nuclease digestion pattern on the secondary structure of DsrA. Pointed (→) and flat (⊥) arrows indicate enhancement or protection, respectively, while the size indicates the degree of change in the digestion pattern (Black, WT; red, Hfq:D9A).

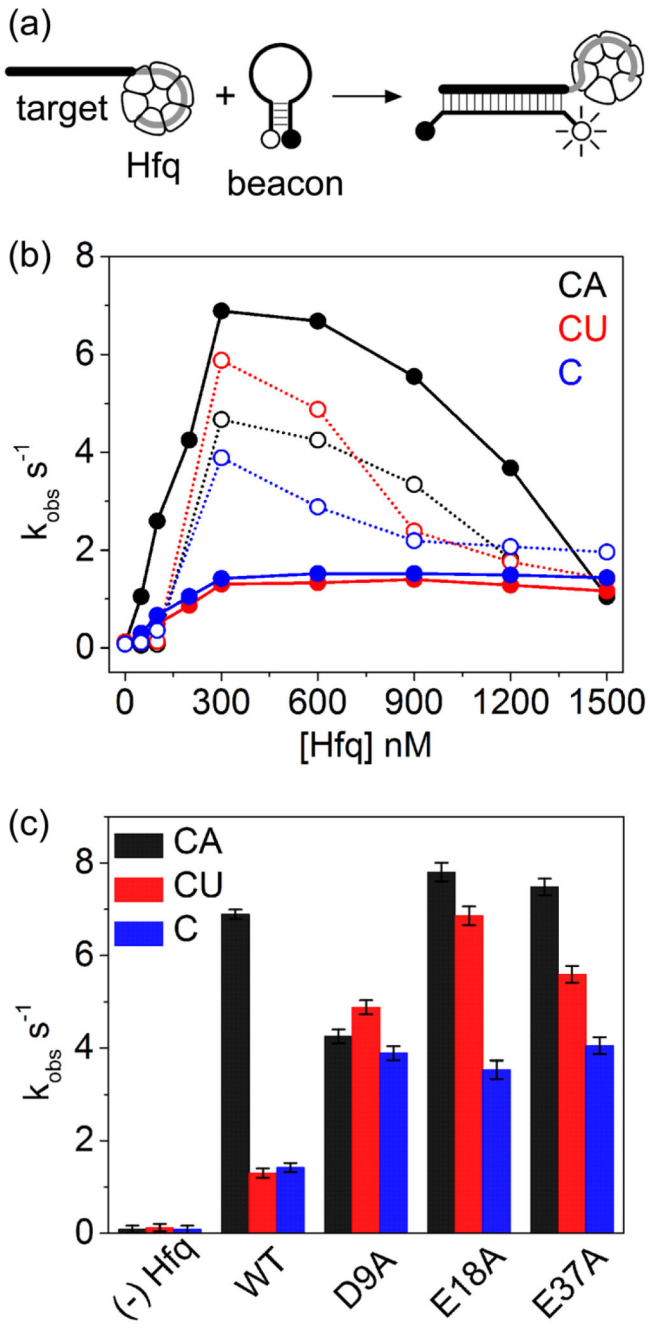

Fig. 4. Acidic residues help discriminate between A-rich and U-rich RNAs

(a) Schematic of molecular beacon annealing assay. (b) Observed annealing rate constants (average of five trials) were plotted against Hfq concentration. Annealing rates were measured by stopped-flow fluorescence using 50 nM molecular beacon, 100 nM target RNA and 0–1500 nM Hfq in TNK at 30°C. WT Hfq, filled circles; Hfq:D9A, open circles. (c) Observed annealing rate constants for Hfq variants (300 nM). Black, A_{18} tail; red, U_6 tail; blue, target sequence only. Results of 5 to 6 trials were averaged; errors bars represent the standard deviation of the mean.

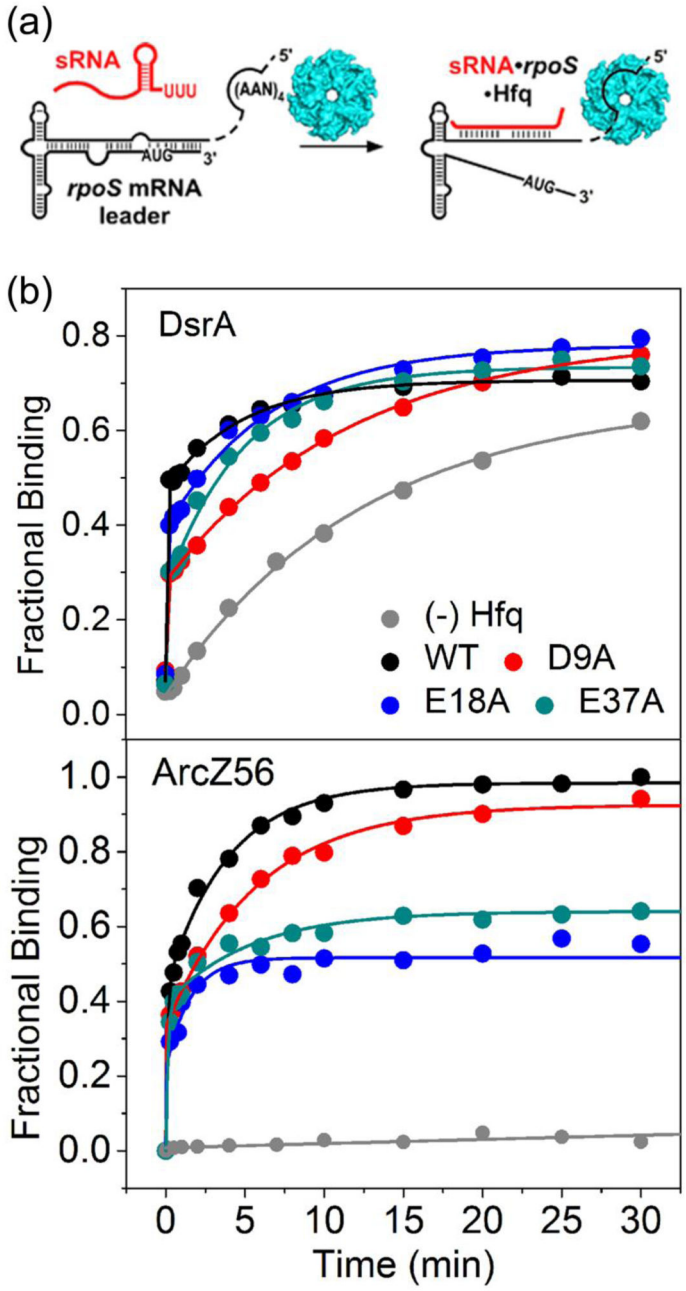

Fig. 5. Acidic side chains promote sRNA and mRNA annealing

(a) Annealing kinetics of ^{32}P-labeled *rpoS301* and 200 nM DsrA or ArcZ56 sRNA with or without 0.6 μM Hfq was measured by native 6% PAGE. (b) Formation of *rpoS*-sRNA-Hfq complexes versus time for DsrA (top) and ArcZ56 (bottom). Grey, no Hfq; black, WT Hfq; red, D9A; blue, E18A; dark cyan, E37A.

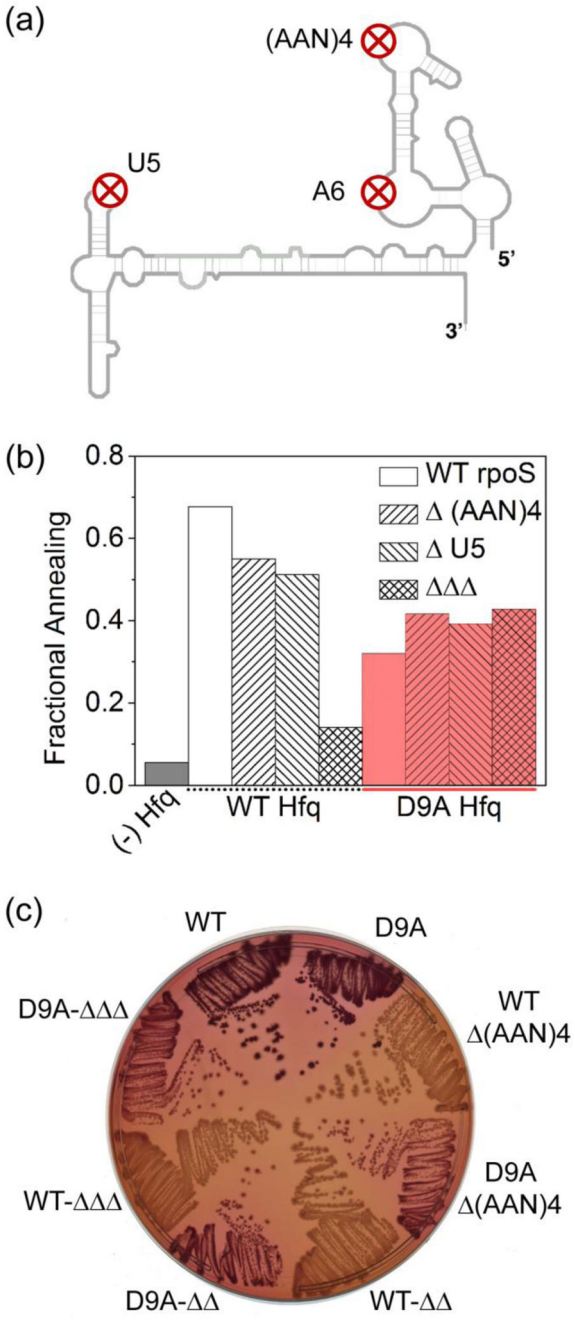

Fig. 6. D9A mutation bypasses an AAN motif in *rpoS* mRNA

(a) Schematic representation of *rpoS* secondary structure and position of Hfq binding sites. (b) Fraction ^{32}P-labeled *rpoS* 301RNA bound to DsrA with or without Hfq after 30 s. Mutations in *rpoS* deleted the upstream AAN motif (Δ(AAN)4), the downstream U_5 loop (ΔU5), or both of these plus an A_6 sequence (ΔΔΔ). (c) *E. coli* cells (Table S1) containing a chromosomal copy of WT or mutant *rpoS::lacZ* fusion, with *hfq*$^+$ or *hfq*D9A alleles in the chromosome for each, were grown overnight at 37 °C on MacConkey agar supplemented with 0.0001% arabinose. Strains used, listed clockwise from WT in Figure, were SG30214,

SG30236 SG30233, SG30242, SG30277, SG30279, DJS3056, and DJS3059, all described in Table S1. Red colonies indicate up-regulation of *lacZ* expression by Hfq and chromosomally derived sRNAs (DsrA, ArcZ and RprA). See Fig. S4 and S5 for further data.

Table 1

Equilibrium binding constant for RNA and Hfq

Hfq variants	K_{D1} (μM)		
	D16-FAM	DsrA sRNA	DsrAΔU6
WT	0.067 ± 0.005	0.22 ± 0.015	1.31 ± 0.1
D9A	0.047 ± 0.002	0.46 ± 0.018	0.67 ± 0.022
E18A	0.024 ± 0.004	0.38 ± 0.02	ND
E37A	ND	0.51 ± 0.021	ND

Overall dissociation constants per Hfq monomer were measured by fluorescence anisotropy (D16-FAM) or native gel mobility shift (DsrA and DsrAΔU6) at 30 °C in TNK buffer. ND, not done. Values are the average and standard deviation from the mean of three independent experiments. The K_d for D16-FAM and WT Hfq is about half that reported for earlier preparations of the protein [18].